CHINESE JOURNAL OF PHYSICS VOL. 34, NO. 5 OCTOBER 1996

# Analytical Potential Energy Curves of Inverse Polynomial Form for Diatomic Molecules : An Application of Two-Step Method to $Li_2$, $Na_2$, NaK, and $K_2$ Molecules

Horng-Tay Jeng and Chen-Shiung Hsue
*Department of Physics, National Tsing Hua University,*
*Hsinchu, Taiwan 300, R.O. C.*

(Received January 23, 1996)

We apply the recently introduced two-step method to the lowest triplet electronic states of the diatomic molecules $Li_2$, $Na_2$, NaK, and $K_2$. The analytical potential energy curves of these states are constructed in the form of inverse polynomial with the experimental vibrational energies as the only inputs. The dissociation energies and the equilibrium constants are also determined. The forms of the interatomic potentials have correct asymptotic behavior in both the short range limit and the long range limit. In contrast to the situations in the widely-used RKR method and also the Dunham type potentials, none of the unphysical inner and outer walls appears in our interatomic potential curves. Based on the potentials obtained, it is predicted that additional unobserved higher vibrational bound states exist for all the systems considered here. This is to be compared with the fact that both the RKR method and the Dunham type potentials have so far failed to predict the existence of the additional bound states for these systems. The described treatments can be applied to other systems as well.

PACS. 31.15.Pf – Variational techniques.
PACS. 33.15.Fm – Bond strengths, dissociation energies.
PACS. 33.20.Tp – Vibrational analysis.

## I. Introduction

One of the most widely used methods to construct the potential energy curves of diatomic molecules from spectroscopic constants is the RKR method [1]. Based on the semiclassical approximation, the RKR method yields directly for each energy level a pair of turning points in the interatomic potentials. However, due to truncation errors and numerical instabilities, it usually results in an unphysical behavior for the inner-wall of the potential, especially for high vibrational levels near the dissociation limit. And various attempts have been devoted to eliminate the unphysical behaviors from the potential energy curves obtained from the RKR method [2,3].

Because of its simplicity, the Dunham type potential [4] is one of the most popular model potentials used to calculate the spectroscopic constants so as to fit the experimental vibrational and rotational levels. Since the Dunham type potential is a polynomial of the internuclear distance $r$, it can effectively describe the behavior of the interatomic potential near the equilibrium point. And usually the low-lying vibration-rotational states can be successfully fitted. However, it has the intrinsic difficulty that it diverges at large internuclear distance and results in an unphysical outer wall for the potential energy curve. **So,** for high vibrational states near the dissociation limit, neither the eigenvalues nor the potential curves can be successfully represented.

In general, it is very difficult to predict the asymptotic behavior of the interatomic potential and the unobserved high lying levels near the dissociation limit by either the Dunham type potential or the RKR method. Recently, we have introduced a two-step method in calculating the vibration-rotational spectrum of diatomic molecules [5-7]. It can deal with effective potentials in a generalized polynomial form such as

$$V_{eff}(r) = \sum_n a_n r^n \tag{1}$$

with $n$ being either positive or negative integers or even arbitrary real numbers. The method can readily be applied to a wide range of potentials including the Lennard-Jones potentials and the Dunham type ones. The effective potential in general consists of a short range repulsive part and a long distance attractive part. The sharp rising repulsive potential core arises from the Coulomb interactions and also from the kinetic energies and the exchanging interactions of the electrons. The long range attractive potential comes mainly from the induced instantaneous dipole-dipole and higher order multipole interactions and behaves asymptotically as $r^{-6}, r^{-8}, \cdots$. Both effects tend to zero as the internuclear distance approaches infinity. In the Lennard-Jones potential, the $r^{-6}$ term was used to describe the asymptotic behavior, and the $r^{-12}$ term was introduced to describe the sharp rising short range behavior. In this work we employ an effective potential of the form (1) with $n = -6, -8, \cdots$, up to -24 for the diatomic molecules $Li_2, Na_2, NaK$, and $K_2$. The form of the interatomic potential is expected to describe correctly the asymptotic behaviors in both long range and short region. This also makes it possible to predict the unobserved high lying vibrational bound levels.

Brief description of this method are presented in section II. In section III, the above algorithm is applied to the molecules Liz [8,9], $Na_2$[10], NaK [II], and $K_2$[12] to find their potential energy curves of the lowest triplet electronic states from the experimental vibrational spectra. The dissociation energies and the equilibrium constants are also presented. To test the predictive power of our method, some of the unobserved higher vibrational levels are given for each system. The conclusions are given in the final section.

## **II.** The **two-step method**

The two-step method is consisted of two main procedures. In the first step, a transformation of domain from the positive half axis of the internuclear distance $r$ to the whole real axis is introduced, and the variational method is applied to the Hamiltonian operator in the second quantization form to find the ground state of the system by algebraic manipulations. In the second step, the ground state energy is improved by a standard diagonalization procedure around the ground state using the harmonic-oscillator basis obtained from the first step. The low-lying excited states are also obtained simultaneously.

The radial part of the Schrödinger equation of the diatomic molecule can be written in atomic units as

$$\left[-\frac{1}{2\mu r^2}\frac{d}{dr}\left(r^2\frac{d}{dr}\right)+V_{eff}(r)\right]\Psi(r)=E\Psi(r), \tag{2}$$

where the effective potential $V_{eff}$ includes both the Coulombic and the centrifugal components and can be written as

$$V_{eff}(r)=V(r)+\frac{l(l+1)}{2\mu r^2}=\sum_n a_n r^n. \tag{3}$$

In order to use the Hermite basis of harmonic oscillator, a transformation of the domain of the internuclear distance $r$ from the positive real axis to the whole real axis is introduced in the first step. A convenient transformation used is

$$r=e^x. \tag{4}$$

The Schrödinger equation becomes

$$\left[-\frac{1}{2\mu}e^{-3x}\frac{d}{dx}\left(e^x\frac{d}{dx}\right)+V_{eff}(x)\right]R(x)=ER(x), \tag{5}$$

with

$$V_{eff}(x)=\sum_n a_n e^{nx}. \tag{6}$$

After the transformation (4), the Hamiltonian is no longer Hermitian. To retain the hermiticity of the Hamiltonian, the following transformation is further introduced.

$$\bar{H}=e^{\frac{3}{2}x}He^{-\frac{3}{2}x}, \qquad \phi(x)=e^{\frac{3}{2}x}R(x). \tag{7}$$

The revised Hamiltonian is now Hermitian and can be written as

$$\bar{H}=-\frac{1}{2\mu}e^{-\frac{3}{2}x}\frac{d}{dx}\left(e^x\frac{d}{dx}e^{-\frac{3}{2}x}\right)+V_{eff}(x). \tag{8}$$

We now expand in terms of the creation and annihilation operators by

$$x=\frac{1}{\sqrt{2\mu\omega}}(a+a^\dagger)+\tau, \qquad \frac{d}{dx}=\sqrt{\frac{\mu\omega}{2}}(a-a^\dagger), \tag{9}$$

with the commutation relations

$$[a,a^\dagger]=1, \qquad [a,a]=0, [a^\dagger,a^\dagger]=0. \tag{10}$$

The two parameters w and $\tau$ are the variational frequency and the displacement of the origin of the harmonic oscillator system respectively. Following procedures described in Ref. [5-7], the Hamiltonian $\bar{H}$ is translated into the second quantized form and is rewritten in a normal ordered form such that all the creation operators are pushed to the left of all the annihilation operators. After some straightforward manipulations, we have

$$\begin{aligned}\bar{H} = & -\frac{\omega}{4}\exp\left(\frac{1}{\mu\omega}-2\tau\right)\exp\left(-\sqrt{\frac{2}{\mu\omega}}a^{\dagger}\right)\left[\left(a^{\dagger}\right)^{2}+a^{2}\right]\exp\left(-\sqrt{\frac{2}{\mu\omega}}a\right)\\ & +\frac{\omega}{2}\exp\left(\frac{1}{\mu\omega}-2\tau\right)\exp\left(-\sqrt{\frac{2}{\mu\omega}}a^{\dagger}\right)[a^{\dagger}a]\exp\left(-\sqrt{\frac{2}{\mu\omega}}a\right)\\ & +\left(\frac{\omega}{4}+\frac{1}{8\mu}\right)\exp\left(\frac{1}{\mu\omega}-2\tau\right)\exp\left(-\sqrt{\frac{2}{\mu\omega}}a^{\dagger}\right)\exp\left(-\sqrt{\frac{2}{\mu\omega}}a\right)\\ & +\textstyle\sum_{n} a_{n}\exp\left(\frac{n^{2}}{4\mu\omega}+n\tau\right)\exp\left(\frac{n}{\sqrt{2\mu\omega}}a^{\dagger}\right)\exp\left(\frac{n}{\sqrt{2\mu\omega}}a\right).\end{aligned} \tag{11}$$

The harmonic oscillator eigenstates

$$a\mid 0>=0, \qquad \mid u>=\frac{(a^{\dagger})^{u}}{\sqrt{u!}}\mid 0> \tag{12}$$

are now taken as the basis with $\mid 0>$ being the trial wave function for the ground state. The expectation value of the trial ground state is

$$\begin{aligned}E_0 &= <0\mid \bar{H}\mid 0>\\ &= \left(\frac{\omega}{4}+\frac{1}{8\mu}\right)\exp\left(\frac{1}{\mu\omega}-2\tau\right)+\textstyle\sum_{n} a_{n}\exp\left(\frac{n^{2}}{4\mu\omega}+n\tau\right).\end{aligned} \tag{13}$$

The variation conditions

$$\frac{\partial E_0}{\partial \tau}=0, \qquad \frac{\partial E_0}{\partial \omega}=0 \tag{14}$$

for the two parameters w and $\tau$ can now be written as

$$\left(\frac{\omega}{2}+\frac{1}{4\mu}\right)\exp\left(\frac{1}{\mu\omega}-2\tau\right)-\sum_{n} na_{n}\exp\left(\frac{n^{2}}{4\mu\omega}+n\tau\right)=0, \tag{15}$$

$$\mu\omega^{2}\exp\left(\frac{1}{\mu\omega}-2\tau\right)-\sum_{n} n(n+2)a_{n}\exp\left(\frac{n^{2}}{4\mu\omega}+n\tau\right)=0 \tag{16}$$

The solutions of $\omega$ and $\tau$ can be obtained by iteration or by standard Newton-Raphson method.

In the second step the ground state energy level is improved by diagonalizing the Hamiltonian matrix in a truncated basis set using Householder or standard Jacobi method [13]. The Hamiltonian matrix elements can be written as

$$
\begin{aligned}
< u \mid \bar{H} \mid v >= & - \frac{\omega}{4} e^{\frac{1}{\mu\omega}-2\tau} < u \mid e^{\alpha_0 a^\dagger} \left[ \left(a^\dagger\right)^2 + a^2 \right] e^{\alpha_0 a} \mid v > \\
& + \frac{\omega}{2} e^{\frac{1}{\mu\omega}-2\tau} < u \mid e^{\alpha_0 a^\dagger} \left[ a^\dagger a \right] e^{\alpha_0 a} \mid v > \\
& + \left( \frac{\omega}{4} + \frac{1}{8\mu} \right) e^{\frac{1}{\mu\omega}-2\tau} < u \mid e^{\alpha_0 a^\dagger} e^{\alpha_0 a} \mid v > \\
& + \sum_n a_n e^{\frac{n^2}{4\mu\omega}+n\tau} < u \mid e^{\beta_n a^\dagger} e^{\beta_n a} \mid v >,
\end{aligned}
\tag{17}
$$

with

$$
\alpha_0 = -\sqrt{\frac{2}{\mu\omega}}, \qquad \beta_n = \frac{n}{\sqrt{2\mu\omega}}. \tag{18}
$$

The matrix elements can be evaluated by using the following identity

$$
< \quad u \,|\, e^{\alpha a^\dagger} \left(a^\dagger\right)^j a^k e^{\alpha a} \,|\, v >= \sum_{q=0}^{u-j} \frac{(u!v!)^{1/2} \alpha^{v+u-k-j-2q}}{(u-j-q)!(v-k-q)!q!}. \tag{19}
$$

By increasing the number of basis, the whole Hilbert space of the wave function can be recovered and the exact eigenvalues can be obtained. The advantage of the two-step approach is that, in general, the rate of convergence is fast and only a small set of basis is needed for the desired accuracy.

## III. Applications

In this section we report an application of the two-step method to construct the potential energy curves of the lowest triplet electronic states of $\mathrm{Li_2}$, $\mathrm{Na_2}$, NaK, and $\mathrm{K_2}$ in inverse polynomial form with the experimental vibrational energies as the only inputs. The potential polynomial starts. with terms of negative integer power $r^{-6}$ to correctly account for the asymptotic behavior of $r^{-6}$(dipole interaction), $r^{-8}$(quadruple interaction), and so on, for the long range potential. Terms of the form $r^{-n}$ with large integer $n$ are used to account for the sharp rising short distance behavior. The correct behavior of the potential at both limit $r \to 0$ and $r \to$ co also affords the additional ability of finding unobserved higher bound vibrational states between the highest observed levels and the dissociation energies. Meanwhile, the equilibrium constant $r_e$ and the dissociation energy $D_e$ are found simultaneously. Atomic units from Ref. [14] are used through out this paper and the values of the masses of the nuclears for all the molecules are based on Ref. [15].

### 111-l. $\mathrm{Li_2}$

The $1^3\Sigma_u^+ - a^3\Sigma_u^+$ transition of $\mathrm{Li_2}$ has been observed via collisionally induced fluorescence with a Fourier-transform spectrometer by Linton *et al.* [8]. Eight vibrational energies of the $\mathrm{Li_2}\, a^3\Sigma_u^+$ state reported in Ref. [8] are used to construct the potential energy curves for $^6\mathrm{Li_2}$ and $^7\mathrm{Li_2}$ in inverse polynomial form (1) with negative integer powers starting with n = -6 up to n = -24. The fitted values of the parameters for the potentials of $^6Li_2$ and $^7Li_2$ together with the corresponding dissociation energies $D_e$, equilibrium constants $r_e$, variational parameters w and $\tau$, and the standard deviations $\sigma$ of the fitting are summarized in Table I. Also listed in the table are the values of the reduced mass $\mu$, the number of parameters np, and the number of energy levels of the vibrational states ne used for fitting. A comparison of the results of the fitted energy levels of $^6Li_2$ and $^7Li_2$ with the experimentally observed energy levels is presented in Table II. We obtained the values (4.2716 A, 4.2635 A) for the equilibrium constants $r_e$ for the $a^3\Sigma_u^+$ state of $^6Li_2$ and $^7Li_2$, respectively. These values are slightly larger than the values (4.1705 Å, 4.1716 A) given in Ref. [8,9]. On the other hand, our dissociation energies $D_e$(333.72 $cm^{-1}$, 333.77 cm-‘ ) for

TABLE I. Potential parameters for the $a^3\Sigma_u^+$state of $^6Li_2$ and $^7Li_2$ molecules. The $np$ parameters are derived from ne states with reduced mass $\mu$. $d$ is the number of basis used. $D_e$, $r_e$ and $\sigma$ are the resultant dissociation energy, equilibrium constant and standard deviation respectively. w and $\tau$ are the variation parameters. The atomic units are used.

| | $^6Li_2$ | $^7Li_2$ |
|---|---|---|
| ne | 8 | 8 |
| $np$ | 11 | 11 |
| $d$ | 70 | 70 |
| $\mu$ | 5482.4495 | 6394.6970 |
| $D_e$ | 0.00152054 | 0.00152077 |
| $r_e$ | 8.07218184 | 8.05688029 |
| $\sigma$ | 0.00000003 | 0.00000002 |
| $w$ | 0.0197194792 | 0.0182484936 |
| $\tau$ | 2.0884238104 | 2.0865264204 |
| $r^0$ | $1.5205403973e-03$ | $1.5207732486e-03$ |
| $r^{-6}$ | $-3.2399799228e+02$ | $-3.2383119112e$ t 02 |
| $r^{-8}$ | $-7.7027052967e+05$ | $-7.7026428560e+05$ |
| $r^{-10}$ | $1.0999711262e+08$ | $1.0999579407e$ t 08 |
| $r^{-12}$ | $5.3177452958e+09$ | $5.3177349499e$ t 09 |
| $r^{-14}$ | $-2.5681887134e+12$ | $-2.5681936237e+12$ |
| $r^{-16}$ | $2.8166203483e+14$ | $2.8166215046e$ t 14 |
| $r^{-18}$ | $-1.6268717793e+16$ | $-1.6268712720e$ t 16 |
| $r^{-20}$ | $5.4095009108e+17$ | $5.4094929434e$ t 17 |
| $r^{-22}$ | $-9.8154767010e+18$ | $-9.8153379628e+18$ |
| $r^{-24}$ | $7.5553608691e+19$ | $7.5549356032e+19$ |

TABLE II. Experimental and theoretical vibrational levels of the $a^3\Sigma_u^+$ state of $^6Li_2$ and $^7Li_2$ molecules in atomic units. There exist at least one and two more unobserved higher bound levels(*) for $^6Li_2$ and $^7Li_2$ molecules separately. The experimental and theoretical dissociation limits $D_e$ are listed at the end of the table.

| $^6Li_2$ | exp . | the. | $^7Li_2$ | exp. | the. |
|---|---|---|---|---|---|
| 0 | **0.00015696** | 0.00015694 | 0 | 0.00014542 | 0.00014542 |
| 1 | 0.00044271 | 0.00044276 | 1 | 0.00041268 | 0.00041266 |
| 2 | 0.00069390 | 0.00069388 | 2 | 0.00064990 | 0.00064994 |
| 3 | 0.00091143 | 0.00091139 | 3 | 0.00085822 | 0.00085821 |
| 4 | 0.00109563 | 0.00109565 | 4 | 0.00103795 | 0.00103791 |
| 5 | 0.00124639 | 0.00124643 | 5 | 0.00118901 | 0.00118902 |
| 6 | 0.00136336 | 0.00136333 | 6 | 0.00131122 | 0.00131125 |
| 7 | 0.00144634 | 0.00144634 | 7 | 0.00140439 | 0.00140437 |
| * |  | 0.0014966 | * |  | 0.00146872 |
|  |  |  | * |  | 0.0015058 |
| $D_e$ | 0.001517 | 0.00152054 | $D_e$ | 0.001517 | 0.00152077 |

the $a^3\Sigma_u^+$ state of $^6Li_2$ and $^7Li_2$ are in good agreement with the values (333 cm$^{-1}$, 333 cm$^{-1}$) reported in Ref. [8,9]. A comparison of our potential energy curves for both $^6Li_2$ and $^7Li_2$ molecules with the RKR [8] and the Dunham type [16] potentials is also presented in Fig. 1 and Fig. 2 respectively. Except near the dissociation region, there are very good agreements among all three potentials: the RKR, the Dunham type and our inverse polynomial potential energy curves. It is interesting to notice from Fig. 1 and Fig. 2 that our potential curves for $^6Li_2$ and $^7Li_2$ almost coincides completely for the whole range, demonstrating the applicability of the adiabatic approximation. As can be seen in the figures, for both $^6Li_2$ and $^7Li_2$ molecules, the Dunham type potential curves turn over beyond the highest RKR outer turning points forming unphysical outer walls. Whereas our inverse polynomial potential energy curves of both $^6Li_2$ and $^7Li_2$ are well-behaved over the whole range. The standard deviations between the reproduced energies and the experimental vibrational spectra turn out to be (0.006 cm$^{-1}$) and (0.004 cm$^{-1}$) for $^6Li_2$ and $^7Li_2$ respectively. Based on the potentials obtained, we predict that there exists at least one and two more unobserved higher bound states between the dissociation energies and the highest levels for $^6Li_2$ and $^7Li_2$, respectively. They are listed at the end of Table II for references and are also shown in Fig. 1 and in Fig. 2. Notice that both the RKR method and the Dunham type potentials were unable to find any additional bound states above the observed ones [8,16].

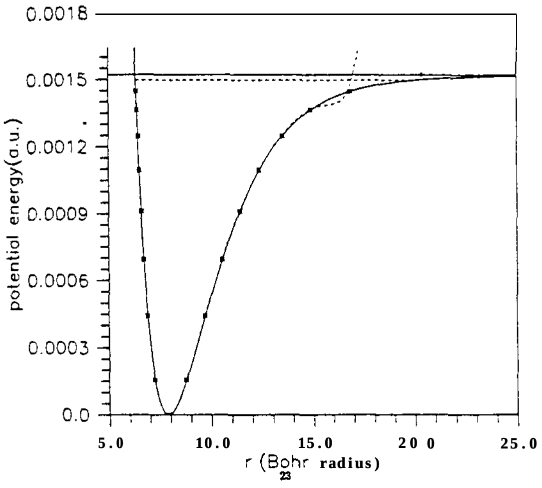

FIG. 1. The resultant curve (solid curve), the RKR (* symbol) [8] and the Dunham type (dashed curve) [16] potential for the $a^3\Sigma_u^+$ state of $^6Li_2$ molecule. The three curves agree well for most region except the outer wall of the Dunham type one. The solid horizontal line is the resultant dissociation energy while the dashed horizontal line is the predicted higher bound level.

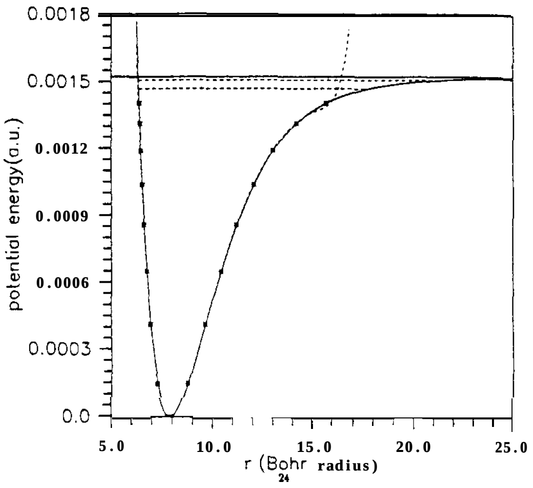

FIG. 2. The resultant curve (solid curve), the RKR (* symbol) [8] and the Dunham type (dashed curve) [16] potential for the $a^3\Sigma_u^+$ state of $^7Li_2$ molecule. The solid horizontal line is the resultant dissociation limit while the two dashed horizontal lines are the predicted higher bound levels.

### 111-2. $Na_2$

The bound vibrational levels of the $Na_2\, a^3\Sigma_u^+$ state have been observed in rotationally resolved fluorescence spectra from single rotation-vibration levels of two $^3\Pi_g$ states by Li et al. [10]. Thirteen vibrational levels of the $Na_2\, a^3\Sigma_u^+$ state reported in Ref. [10] are used as inputs to construct the potential energy curve for $Na_2$ in inverse polynomial form. The fitted parameters of the $Na_2$ $a^3\Sigma_u^+$state are presented in Table III. A comparison of the fitted energy levels of $Na_2$ with the experimentally measured values is presented in Table IV. An equilibrium constant ($r_e=$ 5.1988 Å) for the $Na_2\, a^3\Sigma_u^+$ state is obtained. It is slightly larger than the value (5.0911 Å) given in Ref. [10]. Our dissociation energy $D_e$(174.81 cm-‘ ) for $Na_2$ is in good agreement with the value (174.45 $cm^{-1}$) reported in Ref. [10]. A comparison of our potential energy curve with the RKR [10] and the Dunham type [16] ones for $Na_2$ molecule is presented in Fig. 3. Our curve lies closely to the one obtained by the RKR method over the whole region shown in the figure. The Dunham type potential is constructed from the lower nine states only and does not agree with either the RKR curve or with our curve in the whole region involved. The latter curve turns out to be quite unnature at large internuclear distance and turns over beyond the tenth outer RKR point. Based on our potential energy curve, a further unobserved bound vibrational

TABLE III. Potential parameters for the $a^3\Sigma_u^+$state of $Na_2$ molecule. The $np$ parameters are derived from $ne$ states with reduced mass $\mu$. d is the number of basis used. $D_e$, $r_e$ and $\sigma$ are the resultant dissociation energy, equilibrium constant and standard deviation respectively. w and $\tau$ are the variation parameters. The atomic units are used.

| | $Na_2$ |
|---|---|
| ne | 13 |
| $np$ | 11 |
| $d$ | 100 |
| $\mu$ | 20953.8940 |
| $D_e$ | 0.00079646 |
| $r_e$ | 9.82439763 |
| $\sigma$ | 0.00000132 |
| $w$ | 0.0105198869 |
| $\tau$ | 2.2848688460 |
| $r^0$ | 7.9646472856$e-$ 04 |
| $r^{-6}$ | $-$8.5626509869$e$ + 02 |
| $r^{-8}$ | $-$1.3377654588$e+$ 05 |
| $r^{-10}$ | $-$5.2224714673$e$ + 08 |
| $r^{-12}$ | 2.6608963653$e$ + 11 |
| $r^{-14}$ | $-$5.8778910177$e$ + 13 |
| $r^{-16}$ | 7.4436054901$e$ + 15 |
| $r^{-18}$ | $-$5.7719377449$e$ + 17 |
| $r^{-20}$ | 2.7118549135$e$ + 19 |
| $r^{-22}$ | $-$7.0965567244$e$ + 20 |
| $r^{-24}$ | 7.9438573569$e$ + 21 |

state is predicted to lie very closely to the dissociation limit. It is listed at the end of Table IV and is also shown in Fig. 3. The standard deviation ($\sigma$ = 0.21 $cm^{-1}$) of the resultant potential energy curve of the $Na_2$ molecule is much worse than the cases for the other three molecules. The same situation holds also for the Dunham type potentials [16]. We do not understand the origin of this discrepancy. Further experiments and theoretical studies will clarify this issue.

### 111-3. NaK

Fluorescence spectra of the NaK molecule have been recorded via Fourier-transform

TABLE IV. Experimental and theoretical vibrational levels of the $a^3\Sigma_u^+$ state of $Na_2$ molecule in atomic units. The resultant levels do not match the experimental spectrum well. The unobserved higher bound level(+) is very close to the dissociation limit $D_e$.

| $Na_2$ | exp . | the. |
|---|---|---|
| 0 | 0.0000534 | 0.0000541 |
| 1 | 0.0001612 | 0.0001595 |
| 2 | 0.0002567 | 0.0002571 |
| 3 | 0.0003460 | 0.0003465 |
| 4 | 0.0004257 | 0.0004275 |
| 5 | 0.0005006 | 0.0005000 |
| 6 | 0.0005655 | 0.0005641 |
| 7 | 0.0006218 | 0.0006200 |
| 8 | 0.0006648 | 0.0006677 |
| 9 | 0.0007079 | 0.0007074 |
| 10 | 0.0007389 | 0.0007393 |
| 11 | 0.0007646 | 0.0007635 |
| 12 | 0.0007800 | 0.0007805 |
| * | | 0.000791 |
| $D_e$ | 0.0007949 | 0.0007965 |

spectrometer by Ross et al. [11]. Twelve vibrational energies of the NaK $a^3\Sigma^+$ state reported in Ref. [11] are used here to construct the potential energy curve for NaK molecule in inverse polynomial form. The fitted values of the parameters for the $a^3\Sigma^+$ state of NaK molecule are summerized in Table V. A comparison of the fitted energy levels of the NaK $a^3\Sigma^+$ state with experimentally observed energy levels is presented in Table VI. An equilibrium constant ($r_e = 5.4342$ Å) is obtained for the $a^3\Sigma^+$ state of NaK. The dissociation energy $D_e$ is found to be (208.98 cm$^{-1}$). Both values are in good agreement with the values ($r_e = 5.4385$ Å, $D_e = 209.1$ cm$^{-1}$) reported in Ref. [11]. A comparison of our potential energy curve with the RKR [11] and the Dunham type [16] ones for NaK molecule is presented in Fig. 4. The RKR, Dunham type and inverse polynomial potential curves do not quite agree with each other in most region. Compared with our curve, both the RKR and the Dunham type ones bend a little over in the inner part. Also, the Dunham type potential diverges in the asymptotic region. Our resultant inverse polynomial potential energy curve is well-behaved in both region. The standard deviation between the reproduced energies and the experimental vibrational spectra turns out to be (0.01 cm$^{-1}$) for NaK molecule. Listed at the end of Table VI and also shown in Fig. 4 are three predicted unobserved higher bound levels based on our calculation.

TABLE V. Potential parameters for the a$^3\Sigma$ state of NaK molecule. The $np$ parameters are derived from $ne$ states with reduced mass $\mu.d$ is the number of basis used. $D_e$, $r_e$ and $\sigma$ are the resultant dissociation energy, equilibrium constant and standard deviation respectively. w and $\tau$ are the variation parameters. The atomic units are used.

| | NaK |
|---|---|
| ne | 12 |
| $np$ | 11 |
| d | 80 |
| $\mu$ | 26356.5960 |
| $D_e$ | 0.00095217 |
| $r_e$ | 10.26924529 |
| $\sigma$ | 0.00000007 |
| $\omega$ | 0.0107289310 |
| $\tau$ | 2.3291535344 |
| $r^0$ | $9.5217284966e-04$ |
| $r^{-6}$ | $-5.6437407800e+02$ |
| $r^{-8}$ | $-2.5491313121e+06$ |
| $r^{-10}$ | $7.7829175339e+08$ |
| $r^{-12}$ | $-2.9786057944e+10$ |
| $r^{-14}$ | $-3.7849150108e+13$ |
| $r^{-16}$ | $1.1153501671e+16$ |
| $r^{-18}$ | $-1.5133099585e+18$ |
| $r^{-20}$ | $1.1182289673e+20$ |
| $r^{-22}$ | $-4.3418142692e+21$ |
| $r^{-24}$ | $6.9467670637e+22$ |

### 111-4. **$K_2$**

Several Rydberg triplet states and the a$^3\Sigma_u^+$state have been observed via the perturbation facilitated optical-optical double resonance technique by Li et al. [12]. Eighteen vibrational energies of the $K_2 a^3\Sigma_u^+$ state reported in Ref. [12] are used to construct the potential energy curve for $K_2$ molecule in inverse polynomial form. All the fitted results of the parameters for the a$^3\Sigma_u^+$ state of $K_2$ molecule are summarized in Table VII. A comparison of the fitted energies of the $K_2$ a$^3\Sigma_u^+$state with the experimental observed energy levels is presented in Table VIII. An equilibrium constant ($r_e$ = 5.7935 Å) is obtained for the $a^3\Sigma_u^+$ state of $K_2$ molecule. The value is close to the value (5.7725 A) given in Ref. [12]. Our dissociation energy $D_e$(253.52 cm- ‘ ) is also in good agreement with (254 cm$^{-1}$)

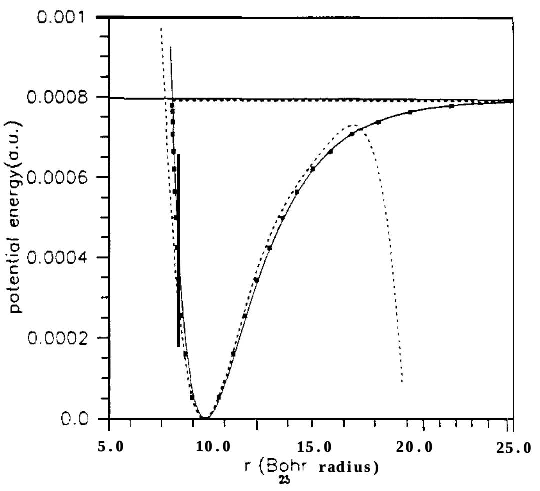

FIG. 3. For the $a^3\Sigma_u^+$ state of $Na_2$ molecule, the resultant curve (solid curve) matches the RKR potential (* symbol) [10] for all thirteen levels much better than the Dunham type (dashed curve) [16] one for the lower nine states. The higher unobserved bound level (dashed horizontal line) is predicted to be very close to the resultant dissociation limit(solid horizontal line).

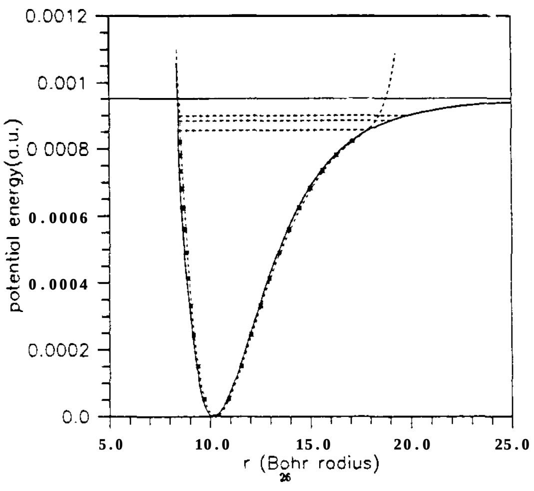

FIG. 4. The resultant curve (solid curve), the RKR (* symbol) [11] and the Dunham type (dashed curve) [16] potential for the $a^3\Sigma^+$ state of NaK molecule. Compared with our curve, the RKR and Dunham type ones bend a little over for inner part, and the Dunham type one diverges in asymptotic region. Between the resultant dissociation energy (solid horizontal line) and the highest observed vibrational level, there exists at least three more bound states(dashed horizontal lines).

reported in Ref. [12]. A comparison of our potential energy curve, the RKR [12] and the Dunham type [16] ones for the $a^3\Sigma_u^+$ state of $K_2$ molecule is presented in Fig. 5. Using refined techniques described in Ref. [17] and Ref. [18], the over bended RKR potential in the unphysical inner wall has been shifted away. Our curve coincides very well with the revised RKR potential for all the vibrational states, while the Dunham type one bends a little over in the inner region and diverges in the outer region. Note that our inverse polynomial potential energy curve is well-behaved in both the short internuclear distance region and the long internuclear distance range. The standard deviation $\sigma$ turns out to he (0.01 cm$^{-1}$) for $K_2$ molecule. Based on the potential energy curve obtained above, it is predicted that there exists at least three higher unobserved bound levels for the $K_2 a^3\Sigma_u^+$ state. They are listed at the end of Table VIII for references and are also shown in Fig. 5. In comparison, both the RKR method and the Dunham type potential were not able to find any additional bound states between the highest observed level and the dissociation limit [12,16].

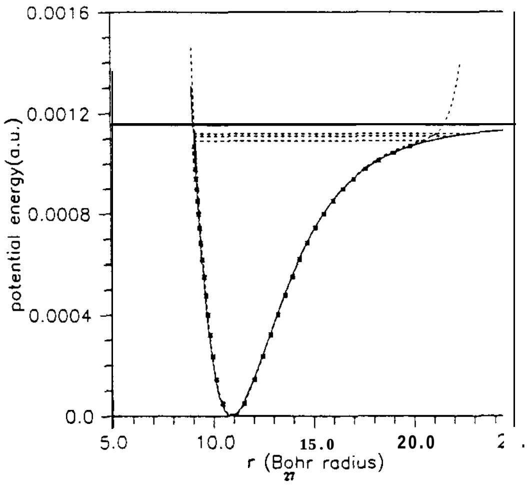

FIG. 5 For the $a^3\Sigma_u^+$ state of $Na_2$ molecule, the resultant curve (solid curve), the RKR (* symbol) [12] and the Dunham type (dashed curve) [16] potential agree well for most region except the outer wall of the Dunham type one. Beneath the resultant dissociation limit (solid horizontal line), three more unobserved higher bound levels (dashed horizontal lines) are obtained.

## IV. Conclusion

As mentioned in Ref. [5] and Ref. [7], the rapid convergence of the two-step calculation is due to the fact that in the second quantization form the variational principle for the "bare" ground state has been carried out analytically in the first step. In addition to the ground state, accurate energies for the low-lying excited states were also obtained in the diagonalization process. The rapid convergence enables us to apply the two-step method to construct the potential energy curves of the diatomic molecules from the experimental vibration-rotational spectrum.

In this paper, a successful application of the two-step method to the diatomic molecules $Li_2, Na_2, NaK$, and $K_2$ has been presented. Expressing the potential energies as polynomials of negative integer powers starting with $n$ = -6, the interatomic potentials have the correct asymptotic behavior in both the short range limit and the long range limit. The leading terms $r^{-6}, r^{-8}$ etc. are used for the $r \rightarrow \infty$ limit while the terms with larger negatives integer powers are used for the $r \rightarrow 0$ limit. The resultant curves produced satisfactory fits for the observed energy levels. They are free of unphysical behavior in the inner and outer walls as are frequently encountered in the widely used RKR method and the Dunham type potentials. Based on the fitted potentials, the existence of at least some higher vibrational bound states are predicted. This is to be compared with the situations in the RKR method and the Dunham type potentials which have failed to find the existence of these states.

TABLE VI. Experimental and theoretical vibrational levels of the NaK $a^3\Sigma^+$ state in atomic units. There are at least three higher unobserved bound levels(*) for NaK molecule. The last line are the dissociation limits $D_e$.

| NaK | exp. | the. |
|---|---|---|
| 0 | 0.0000517 | 0.0000518 |
| 1 | 0.0001508 | 0.0001507 |
| 2 | 0.0002442 | 0.0002442 |
| 3 | 0.0003319 | 0.0003320 |
| 4 | 0.0004139 | 0.0004139 |
| 5 | 0.0004899 | 0.0004899 |
| 6 | 0.0005602 | 0.0005601 |
| 7 | 0.0006246 | 0.0006245 |
| 8 | 0.0006830 | 0.0006830 |
| 9 | 0.0007354 | 0.0007355 |
| 10 | 0.0007818 | 0.0007819 |
| 11 | 0.0008222 | 0.0008221 |
| * |  | 0.0008563 |
| * |  | 0.000885 |
| * |  | 0.00091 |
| $D_e$ | 0.0009527 | 0.0009522 |

Based on the fitted potential, we have predicted the existence of one additional vibrational level with energy of 0.0014966 a.u. for the $a^3\Sigma_u^+$ state of $^6$Li$_2$ and two levels of 0.00146872, 0.0015058 a.u. for $^7$Li$_2$ below the dissociation limit which is 0.00152 a.u.. The wave functions of these states extend beyond 20 and 18, 21 $a_0$ (Bohr-radius) respectively. As mentioned in Ref. [8] that one of the main experimental difficulties of finding these higher vibrational levels in the experiments for Li$_2$ come from the very intense $A^1\Sigma_u^+ - X^1\Sigma_g^+$ transitions. For Na$_2$, we have predicted an additional higher vibrational level with energy of 0.00791 a.u. which is very close to the ionization limit 0.007965 a.u.. In the mean time, the wave function extends far beyond 25 $a_0$ for this vibrational state. This long range wave function poses a challenging problem for the experimental observation. In the case of NaK, we predict three additional levels : 0.0008563, 0.000885, and 0.00091 a.u. which are considerably beneath the dissociation energy 0.0009522 a.u.. The wave functions of these states are limited within 20 $a_0$ and these vibrational levels may perhaps easier be observed experimentally. Similarly, for K$_2$, the three predicted levels are 0.0010914, 0.001110, and 0.00112 a.u. below the dissociation limit of 0.00115514 a.u.. The wave functions of these higher states extend to 21 $\sim$ 23 an. It is hoped that our work will stimulate further experimental works to confirm the existence of these states.

TABLE VII. Potential parameters for the $a^3\Sigma_u^+$state of $K_2$ molecule. The $np$ parameters are derived from $ne$ states with reduced mass $\mu$. d is the number of basis used. $D_e, r_e$ and $\sigma$ are the resultant dissociation energy, equilibrium constant and standard deviation respectively. w and $\tau$ are the variation parameters. The atomic units are used.

| | $K_2$ |
|---|---|
| ne | 18 |
| $np$ | 11 |
| d | 120 |
| $\mu$ | 35513.2475 |
| $D_e$ | 0.00115514 |
| $r_e$ | 10.94810346 |
| $\sigma$ | 0.00000006 |
| $w$ | 0.0116102390 |
| $\tau$ | 2.3931662416 |
| $r^0$ | $1.1551362066e-03$ |
| $r^{-6}$ | $-1.4375301751e+03$ |
| $r^{-8}$ | $-4.7910072130e+06$ |
| $r^{-10}$ | $2.5890012647e+09$ |
| $r^{-12}$ | $-8.2133399765e+11$ |
| $r^{-14}$ | $1.5948627059e+14$ |
| $r^{-16}$ | $-1.6743862483e+16$ |
| $r^{-18}$ | $6.5982050861e+17$ |
| $r^{-20}$ | $3.1075412732e+19$ |
| $r^{-22}$ | $-3.8004004047e+21$ |
| $r^{-24}$ | $9.9809541796e+22$ |

As an indication for the predictive power of this method, we have also fitted the interatomic potential of $^6Li_2$ with the lower 7 states instead of 8 observed levels. With this potential, we then calculate the energy levels of the 8th and 9th vibrational states. The 8th level generated from the lower 7 states has an energy of 0.00144636 a.u. which is 2 x $10^{-8}$ a.u. higher than the experimental value of 0.00144634 a.u.. This small deviation is to be compared with the value of the 8th vibrational state well fitted with the experimental data within this work as shown in Table II. For the 9th level, the predicted values are 0.00149662 a.u. and 0.00149664 a.u. obtained from the lower 8 and 7 states respectively. Thus the accuracy for the predicted 9th excited vibrational level of $^6Li_2$ is about 2 x $10^{-8}$ a.u. which corresponds to an error of 1.3 x $10^{-5}$ and is a successful demonstration of the possible predictive power of this method.

TABLE VIII. Experimental and theoretical vibrational levels of the $K_2\, a^3\Sigma_u^+$ state in atomic units. There are at least three higher unobserved bound levels(*) under the dissociation limit $D_e$ for $K_2$ molecule.

| $K_2$ | exp. | the. |
|---|---|---|
| 0 | 0.000048923 | 0.000048860 |
| 1 | 0.000143204 | 0.000143274 |
| 2 | 0.000233203 | 0.000233254 |
| 3 | 0.000318919 | 0.000318925 |
| 4 | 0.000400353 | 0.000400326 |
| 5 | 0.000477503 | 0.000477462 |
| 6 | 0.000550370 | 0.000550331 |
| 7 | 0.000618954 | 0.000618930 |
| 8 | 0.000683256 | 0.000683255 |
| 9 | 0.000743275 | 0.000743301 |
| 10 | 0.000799010 | 0.000799060 |
| 11 | 0.000850463 | 0.000850522 |
| 12 | 0.000897633 | 0.000897675 |
| 13 | 0.000940520 | 0.000940518 |
| 14 | 0.000979124 | 0.000979060 |
| 15 | 0.001013445 | 0.001013336 |
| 16 | 0.001043483 | 0.001043409 |
| 17 | 0.001069238 | 0.001069378 |
| * |  | 0.0010914 |
| * |  | 0.001110 |
| * |  | 0.00112 |
| $D_e$ | 0.00115512 | 0.00115514 |

The weakest point in the approach here is the behavior of the interatomic potentials in the deep well around the equilibrium internuclear positions of the molecules. It is artificially generated by a cancellation of competing terms of pure negative power form which can correctly describe the behavior in the short and the long range region. The resultant potential curves are expected to be difficult in an accurate description of the behavior of the interatomic potential near the equilibrium internuclear distance. Thus the values of the equilibrium positions obtained here will be the least accurate ones among the results presented here.

Note that the two-step method could readily be applied to the Dunham type potentials thus achieving very accurate potential energy curves near the equilibrium positions, but at the expense of the appearance of the intrinsic divergence behavior in the $r \rightarrow \infty$ region like the Dunham type potentials. But here we have the advantage that the method can be easily generalized to more complicated molecular systems such as triatomic molecules or other polyatomic molecules as well. Such applications will be presented in the future. The results of this work demonstrates that this method is a powerful tool in dealing with the vibration-rotational spectrum of diatomic molecules.

## Acknowledgment

This work was supported by the National Science Council of the Republic of China (No. 836007B045).

## References

[1] R. Rydberg, Z. Physik 73, 367 (1931); 0. Klein, *ibid*, 76, 226 (1932); A. L. G. Rees, Proc. Roy. Soc. **A59, 998 (1947).**
[2] J. M. Hutson, J. Phys. B14, 851 (1981).
[3] P. Pajunen, J. Chem. Phys. 92, 7484 (1990).
[4] J. L. Dunham, Phys. Rev. 41, 721 (1932).
[5] P. Chang and C.-S. Hsue, Phys. Rev. **A49,** 4448 (1994).
[6] C.-S. Hsue, Chin. J. Phys. 32, 821 (1994).
[7] C.-S. Hsue and J. L. Chern, Phys. Rev. **D29,** 643 (1984).
[8] C. Linton, T. L. Murphy, F. Martin, R. Bacis, and J. Verges, J. Chem. Phys. 91, 6036 (1989).
[9] F. Martin, R. Bacis, J. Verges, C. Linton, G. Bujin, C. H. Cheng, and E. Stad, Spectrochimica Acta A44, 1369 (1988).
[10] L. Li, S. F. R'ice, and R. W. Field, J. Chem. Phys. 82, 1178 (1985).
[11] A. J. Ross, C. Effantin, J. d'Incan, and R. F. Barrow, Mol. Phys. 56, 903 (1985).
[12] L. Li, A. M. Lyyra, W. T. Luh, and W. C. Stwalley, J. Chem. Phys. 93, 8452 (1990).
[13] W. H. Press, S. A. Teukolsky, W. T. Vetterling, and B. P. Flannery, *Numerical Recipes in C* (Cambridge, University Press, 1992), pp. 412-420.
[14] E. R. Cohen and B. N. Taylor, Phys. Today **BG9**, (1993).
[15] C. M. Lederer and V. S. Shirley, *Table of Isotopes* (Wiley, New York, 1978).
[16] C. G. Diaz, W. T. Luh, F. M. Fernandez, Chin. J. Phys. **31**, 391 (1993).
[17] S. C. Yang, J. Chem. Phys. 77, 2884 (1982).
[18] W. T. Zemke and W. C. Stwalley, Chem. Phys. Lett. 143, 84 (1988).